

# Modelling and simulation of the grounding system of a class of power transmission line towers involving inhomogeneous conductive media



E. Faleiro<sup>a,\*</sup>, G. Asensio<sup>a</sup>, J. Moreno<sup>a</sup>, P. Simón<sup>b</sup>, G. Denche<sup>a</sup>, D. García<sup>a</sup>

<sup>a</sup> Polytechnic University of Madrid (UPM), Escuela Técnica Superior de Ingeniería y Diseño Industrial (ETSIDI), Ronda de Valencia 3, 28012 Madrid, Spain

<sup>b</sup> LCOE Laboratory, Calle Diesel 13. P.I. El Lomo, 28906 Madrid, Spain

## ARTICLE INFO

### Article history:

Received 16 March 2015

Received in revised form 2 December 2015

Accepted 17 February 2016

### Keywords:

Power transmission line towers

Electromagnetic-based grounding analysis

Inhomogeneous soils

Equivalent surface charge distributions

## ABSTRACT

The grounding system of a class of power transmission line towers involving inhomogeneous conductive media is modelled in order to simulate its behaviour in case that a current earth fault takes place. The simulation includes structural elements of the tower and provides an estimate of the grounding resistance of the tower, assuming that a standard grounding electrode is buried as the main part of the grounding installation. The effect of structural elements on grounding resistance is discussed and a quantitative estimate of this effect is evaluated.

© 2016 Elsevier B.V. All rights reserved.

## 1. Introduction

Certain types of towers for power transmission lines are installed in the ground with a foundation that is introduced into the soil to a significant depth, containing a part of the metallic tower structure, all forming a compact cubic block of concrete in contact with the conductive surrounding soil. Standard grounding electrodes are used as the main part of the grounding system, adapting their type and form to the operating range of the power line [1]. Finally, to avoid high potential gradients that would occur near the tower in case of current fault, an “equipotential platform” is usually added around the tower, which consists of a platform made of concrete, inside which a metallic grid is placed. This grid is usually connected to the metallic structure of the tower itself, the latter being electrically connected to the grounding electrode buried into the soil. The result is a flattening of the contact potential profile on the platform in case of fault. However, the grounding system of the tower has become complex because it consists of a set of three interconnected conductors, which are immersed in conductive media of different nature and properties, namely, on the one hand, the metallic grid of the platform and the metallic structure of the tower, that are forming a regular concrete block sunk into the ground, and on the other hand, the grounding electrode buried into the soil. The objective is to simulate in a suitable manner a system consisting of three electrodes, two of which are

immersed in a finite volume of material which has low electrical conductivity such as concrete, which in turn is surrounded by a semi-infinite volume of material with higher conductivity, where the third electrode is placed, that is, the soil. The three electrodes are interconnected so as to have the same electric potential. Thus, the effect of the platform and the tower foundations on the grounding resistance of the tower can be appropriately studied.

The analysis of grounding systems buried in soils composed of finite volumes of different conductivities such as the system of electrodes placed in different electric media appearing in this paper, falls into the problems studied by electromagnetism in inhomogeneous media [2,3]. When the semi-infinite medium is composed of horizontal or vertical layers of infinite extension, the image theory and similar approaches can be applied to find an approximate solution [4–6]. In this case, it is not possible to do so, because the interface between the two existing electrical media, though fairly regular, is not layered, but instead is composed of finite volumes of different conductivities.

In this paper, we will address the problem through the so-called equivalent surface charge distributions (ESCD) [7,8], which proposes to replace the influence of the interface between the different electrical media for surface current distributions to the surrounding medium, so that the boundary condition is satisfied at the interface, namely, the conservation of the normal component of the interface surface of the current density  $J_{1n} = J_{2n}$ ,  $\vec{n}$  being the unitary normal vector to the interface when crossing from medium 1 to medium 2.

\* Corresponding author. Tel.: +34 913367686; fax: +34 3366850.  
E-mail addresses: [eduardo.faleiro@upm.es](mailto:eduardo.faleiro@upm.es), [efalus@gmail.com](mailto:efalus@gmail.com) (E. Faleiro).

Although the ESCD was originally applied to calculate capacitances [9–11], the method, with some modifications, will be used in this paper to calculate the current delivered by each electrode and the common potential to all of them, being able to eventually estimate the grounding resistance of the tower composed by the three electrodes previously described. The dependency on the tower grounding resistance with the ratio between the conductivities of the two involved media will be also investigated. As an application, the resistivity changes associated spatial and temporal variability [12] of soil and structural elements on the grounding resistance can be evaluated through the aforementioned ratio.

With this general approach, the paper is organized as follows: After the introduction to the problem in this section, the theoretical foundation and calculation scheme that has been used is developed in Section 2. In Section 3, the complete modelling of the tower grounding system and the numerical procedure used to find an approximate solution to the problem is presented. Results and recommendations for a better design adapted to the actual conditions of such towers are addressed in Section 4. Finally, the conclusions of this work are summarized in Section 5.

## 2. Theoretical background

The problem of finding the potential profile, step, touch and mesh voltages created by a system of conductors in mutual interaction, immersed in an electrically inhomogeneous medium can essentially be solved by finding a solution of

$$\vec{\nabla} \cdot (\sigma(\vec{r}) \cdot \vec{\nabla} \phi(\vec{r})) = 0 \quad (1)$$

where,  $\sigma(\vec{r})$  is the conductivity function and  $\phi(\vec{r})$  the potential that satisfies a set of boundary conditions which define univocally the configuration of the conductors, their electrical state and the properties of the inhomogeneous medium.

We assume that there exist  $N_C$  conductors of surfaces  $S_{C_i}$ , located in a semi-infinite medium horizontally bounded by the ground surface G. It is assumed that the whole semi-infinite medium is globally inhomogeneous, but consists of  $N_R$  finite size volumes of constant conductivity and surface  $S_{I_j}$ , immersed in a homogeneous semi-infinite medium of different conductivity, as is schematically illustrated in Fig. 1.

The conductors may be independent or electrically interconnected. For each region R where, conductivity is a constant, the equations that needs to be solved are

$$\begin{aligned} \Delta \phi_R &= 0 \\ \phi_R(\vec{r})|_{\vec{r} \in S_{C_i}} &= V_i \\ \vec{n} \cdot \vec{\nabla} \phi_R|_G &= 0 \\ \phi_R(\vec{r})|_{S_1} &= \phi_{R'}(\vec{r})|_{S_1} \\ \sigma_R \vec{\nabla} \phi_R(\vec{r}) \cdot \vec{n}|_{S_1} &= \sigma_{R'} \vec{\nabla} \phi_{R'}(\vec{r}) \cdot \vec{n}|_{S_1} \end{aligned} \quad (2)$$

The last two equations in Eq. (2) express the continuity of both the electric potential and the current density flow through the interface  $S_1$ , separating the R and R' regions of constant conductivities  $\sigma_R$  and  $\sigma_{R'}$ . The vector  $\vec{n}(\vec{r})$  is a unitary vector normal to  $S_1$  along R–R'.

Using the second Green identity, Eq. (2) can be converted to an integral form where the sources of the potential  $\phi_R$  are surface current distributions on all the conductors of the system  $\lambda_{C_i}$ , and surface current distributions  $\lambda_{I_j}$  on all the interfaces  $I_j$ , separating regions of different conductivity, the core of the ESCD approach

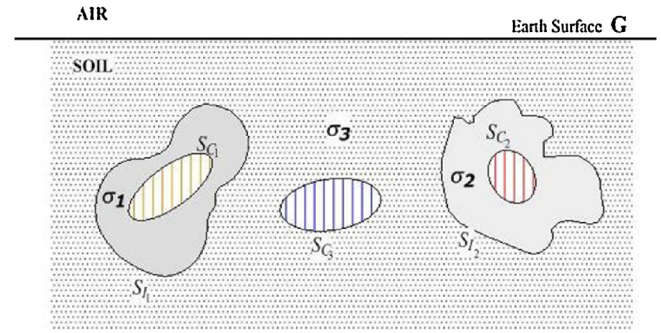


Fig. 1. Pictorial representation of a complex system of interacting electrodes in an inhomogeneous piece-wise medium.

[7–11],

$$\begin{aligned} \phi(\vec{r}) &= \sum_i \int_{S_{C_i}} \frac{\lambda_{C_i}(\vec{r}_i) dS_i}{4\pi\sigma_i |\vec{r} - \vec{r}_i|} + \sum_j \int_{S_{I_j}} \frac{\lambda_{I_j}(\vec{r}_j) dS_j}{4\pi k_j |\vec{r} - \vec{r}_j|} \quad i = 1, \dots, N_C; \\ & \quad j = 1, \dots, N_I \end{aligned} \quad (3)$$

where,  $N_C$  is the number of conductors in the system and  $N_I$  is the number of different interfaces separating the different conductive media.

Eq. (3) is valid for all the regions R where, the conductivity  $\sigma_i$  is a constant and  $k_j$  is given by  $k_j = \sigma_+ \sigma_- / (\sigma_+ - \sigma_-)$ , where,  $\sigma_-$  and  $\sigma_+$  account for conductivities at both sides of the interface  $I_j$ .

The surface current distributions  $\lambda_{C_i}$  and  $\lambda_{I_j}$  can be calculated by imposing the boundary conditions on all the conductor surfaces  $S_{C_i}$  and density current fluxes continuity along all the interfaces  $S_{I_j}$

$$\begin{aligned} \phi(\vec{r})|_{S_{C_i}} &= V_i \quad i = 1, \dots, N_C \\ \sigma_-(\vec{r}) \vec{\nabla} \phi_-(\vec{r}) \cdot \vec{n}|_{S_1} &= \sigma_+(\vec{r}) \vec{\nabla} \phi_+(\vec{r}) \cdot \vec{n}|_{S_1} \end{aligned} \quad (4)$$

where, symbols subscripted with + and – denote the values on either side of the interface and the unitary normal vector  $\vec{n}$  pointing from region – to region +. The continuity of current density flux through the interface surface separating the two media, as expressed by the last Eq. (4), means that although the potential is continuous in the interface, the normal component of the potential gradient at the interface surface is discontinuous. The discontinuity can be expressed by the following equation [7–11],

$$\begin{aligned} \frac{\lambda_{I_j}(\vec{r})}{k_j} + 2K \left[ \sum_i \int_{S_{C_i}} \frac{\lambda_{C_i}(\vec{r}_i)}{4\pi\sigma_i} \vec{\nabla} \left( \frac{1}{|\vec{r} - \vec{r}_i|} \right) \cdot \vec{n} dS_i \right. \\ \left. + \sum_j \int_{S_{I_j}} \frac{\lambda_{I_j}(\vec{r}_j)}{4\pi k_j} \vec{\nabla} \left( \frac{1}{|\vec{r} - \vec{r}_j|} \right) \cdot \vec{n} dS_j \right] = 0 \\ i = 1, \dots, N_C; \quad j = 1, \dots, N_I \end{aligned} \quad (5)$$

where, point  $\vec{r}$  belongs to the  $I_j$  interface and point  $\vec{r}_j = \vec{r}$  is excluded in the integrand of the second integral term of Eq. (5). The prefactor K is defined by  $K = \frac{\sigma_+ - \sigma_-}{\sigma_+ + \sigma_-}$ , where, as before,  $\sigma_-$  and  $\sigma_+$  account for conductivities at both sides of the interface  $I_j$ . Note that for convenience, in this theoretical framework the variables  $\frac{\lambda_{C_i}}{\sigma_i}$  and  $\frac{\lambda_{I_j}}{k_j}$  ( $\text{A } \Omega \text{ m}^{-1}$ ) are chosen as unknowns to be computed, but the really important variables are the densities  $\lambda_{C_i}$  and  $\lambda_{I_j}$  ( $\text{A m}^{-2}$ ).

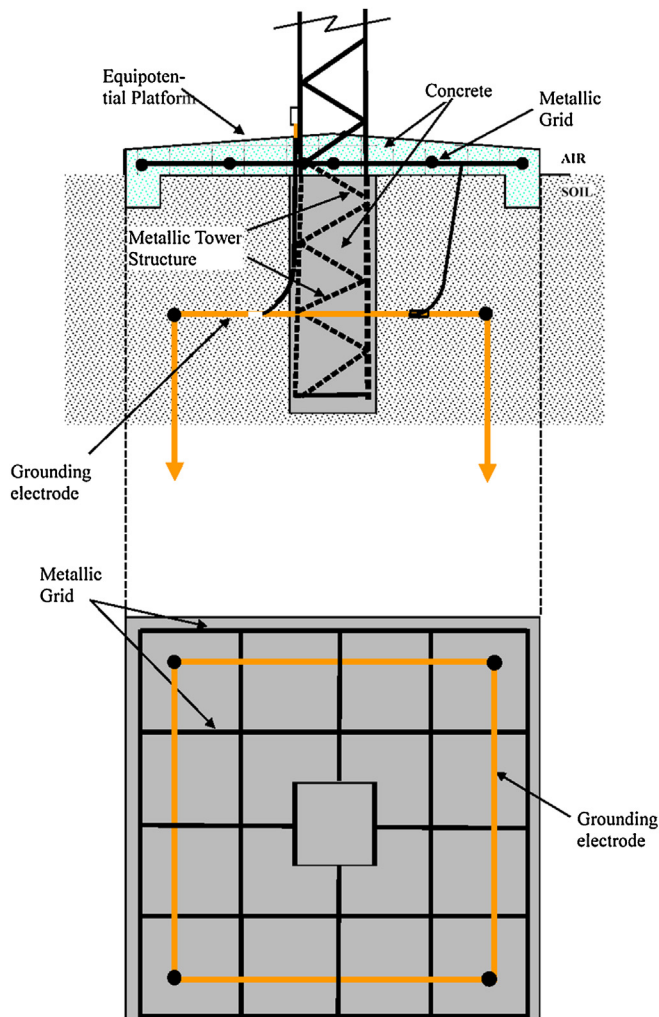


Fig. 2. Grounding system of the transmission line tower as is theoretically designed (left panel). An image of an experimental tower is shown in the right panel.

### 3. Modelling the tower grounding system

The actual grounding system configuration of the towers that are the object of this study are shown in the two panels of Fig. 2. They show two structural elements of the tower that are: (A) foundations, penetrating the soil, which contains a part of the tower metallic structure, all in a cubic shaped concrete block, (B) a horizontal platform at ground level, which contains a meshed flat metallic structure, that is electrically connected to the ground electrode and also made of a cubic block of concrete. This platform will be referred to as equipotential platform, because, as will be seen later, it flattens the ground potential rise due to a current flowing to the ground.

The two structural elements described above constitute the volume medium  $\mathbf{M}_1$ , of finite size and characterized by a low conductivity, completely surrounded by the volume medium  $\mathbf{M}_2$ , the semi-infinite ground of moderate conductivity. The type of platform and the grounding electrode of this class of towers are being used in the framework of the TABÓN Project, a research project sponsored by the companies Iberdrola Distribución, Iberdrola S.A. and ATISAE, and funded by the EEA grants and Norway Grants.

Together with the structural elements, Fig. 2 also shows the grounding electrode in the volume medium  $\mathbf{M}_2$ . The grounding electrode could be characterised by knowing the normalized parameter  $K_r = V/I\rho$ , where,  $V$  is the potential acquired by the

electrode when a current  $I$  flows to a homogeneous soil of resistivity  $\rho$ . In this work, the grounding electrode, which is shown in detail in Fig. 3, has a value of  $K_r = 0.1226 \text{ m}^{-1}$ , which means that, for example, in a homogeneous soil of  $200 \Omega \text{ m}$  and assuming that this is the only electrode, would offer an electrical resistance of  $24.51 \Omega$ . This value of  $K_r$  has been obtained by various methods, including commercial software. In particular, the same result is obtained by applying the algorithm used in this work by imposing that  $\rho_1 = \rho_2 = 200 \Omega \text{ m}$  to the system composed only by the grounding electrode, excluding others.

In summary, we have three metallic conductors, two of them in the resistive medium  $\mathbf{M}_1$  composed of concrete with resistivity  $\rho_1$ , and the third in the resistive medium  $\mathbf{M}_2$ , the soil, with resistivity  $\rho_2$ , all electrically interconnected, delivering to the ground a low frequency electric current  $I$ . The interface separating the two conducting media is the surface contact between the concrete blocks and the ground. Typical values for resistivity in the frame of the TABÓN Project are  $\rho_1 = 3000 \Omega \text{ m}$  and  $\rho_2 = 200 \Omega \text{ m}$ . However, in this paper, we will study the dependence of the grounding resistance with the ratio between the values of the concrete and soil resistivity. For this purpose, we introduce the dimensionless parameter  $K_\rho = \rho_1/\rho_2$  and set  $\rho_2 = 1 \Omega \text{ m}$  and  $I = 1 \text{ A}$ , which allows a much clearer evaluation of the effect of the tower structural elements by changing the value of  $K_\rho$ .

The parameter to be varied is the ratio  $K_\rho$ , and the normalized potential  $K_V = V/\rho_2 I$  is calculated so that the grounding

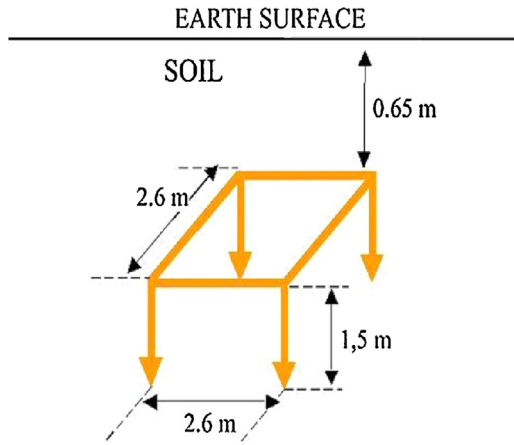


Fig. 3. Grounding electrode details.

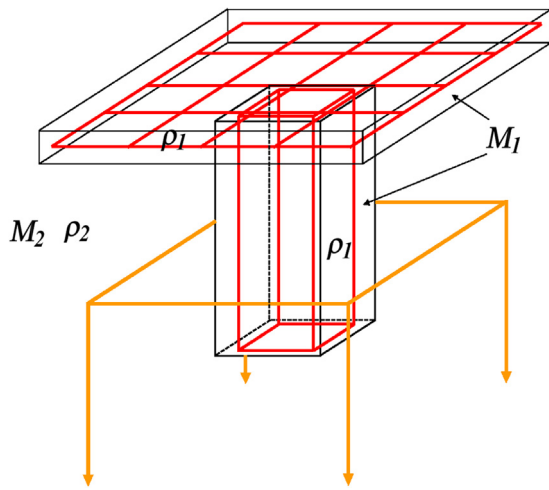


Fig. 4. The model of the grounding system of the transmission line tower. Finite volume material  $M_1$  has resistivity  $\rho_1$  and semi-infinite volume  $M_2$  has resistivity  $\rho_2$ .

resistance  $R$  is obtained by multiplying the normalized potential value  $K_V$  associated to the ratio  $K_\rho$  by soil resistivity  $\rho_2$ ,  $R = K_V \rho_2$ . It should be noted that  $K_V$  matches the previously introduced parameter  $K_r$  when  $\rho_1 = \rho_2$  that is, when the soil is homogeneous.

The modelling of the system described above is performed as shown in Fig. 4. The platform and the foundation are replaced by two parallelepiped of concrete, the medium  $M_1$ , inside which the metallic grid and part of the tower metallic structure are replaced by a thin wire structure [13]. The grounding electrode in the medium  $M_2$  is also modelled as a conductive thin wire structure with the actual shape and size. Fig. 5 is a view of the model from a vertical plane including a view of the platform with the metallic grid. In the figure, the main lengths to be used in the simulation are included. The metallic grid is located at the geometric centre of the platform. Note that for simplicity, the upper side of the platform model has been placed at ground level. For this type of tower, this does not introduce significant changes in the calculated values, otherwise it would greatly complicate the calculations because the theory of images for treating soil interface cannot be used.

Thin wires are easy to model as they allow to simplify many of the formulas used in this paper. Thus, as in Eqs. (3) and (5), the integrals over the conductive surfaces can be replaced by integration along the axis of the thin wires [13]. The sources are now current

densities  $\lambda_{L_i}$  along the wire axis. In summary, the equations to be solved with these approximations are,

$$V_i(\vec{r}) = \sum_i \int_{L_i} \frac{\lambda_{L_i}(\vec{r}_i) dL_i}{4\pi\sigma_i |\vec{r} - \vec{r}_i|} + \sum_j \int_{I_j} \frac{\lambda_{I_j}(\vec{r}_j) dS_j}{4\pi k_j |\vec{r} - \vec{r}_j|} \quad i = 1, \dots, N_C; \\ j = 1, \dots, N_I$$

$$\frac{\lambda_{I_j}(\vec{r})}{k_j} + 2K \left[ \begin{array}{l} \sum_i \int_{L_i} \frac{\lambda_{L_i}(\vec{r}_i)}{4\pi\sigma_i} \vec{\nabla} \left( \frac{1}{|\vec{r} - \vec{r}_i|} \right) \cdot \vec{n} \cdot dL_i + \\ \sum_j \int_{I_j} \frac{\lambda_{I_j}(\vec{r}_j)}{4\pi k_j} \vec{\nabla} \left( \frac{1}{|\vec{r} - \vec{r}_j|} \right) \cdot \vec{n} \cdot dS_j \end{array} \right] = 0 \\ i = 1, \dots, N_C; \quad j = 1, \dots, N_I \quad (6)$$

where,  $V_i(\vec{r})$  is the potential at any point  $\vec{r}$  on the surface of the thin wire  $L_i$ . Eq. (6) states that there are  $N_C$  equations for conductor potentials and  $N_I$  equations for the different interfaces present in the medium. In the proposed model, there are three equations for the potentials of the three conductors and one equation for the interface of the two considered conductive media.

The solution of Eq. (6) is found by using the Method of Moments (MoM) [13,14], by carrying out a segmentation of the thin wire axis and a triangular meshing of the interface. In this scheme of calculation, current densities  $\lambda_{L_{i,j}}$  and surface current densities  $\lambda_{I_t}$  associated respectively with the thin wire axis segments and the triangular patches on the interface, are supposed constant. As an example, Fig. 6 shows a picture of the structure meshing, including all the involved conductors, when  $N_{tri} = 1852$  pieces. Using as weight functions Dirac Delta type functions, a linear system is obtained in the unknowns  $\lambda_{L_{i,j}}$  and  $\lambda_{I_t}$ , which are the current densities previously introduced.

For the proposed model in this paper, if each electrode is divided into  $M_{L_i}$  segments ( $i = 1, \dots, 3$ ) and the interface consist of  $M_S$  triangular patches, Eq. (6) is written as

$$V_{i,j} = \sum_{n,m} \lambda_{L_{n,m}} \int_{L_{n,m}} \frac{dL_{n,m}}{4\pi\sigma_n |\vec{r}_{i,j} - \vec{r}_{n,m}|} + \sum_t \lambda_{I_t} \int_{I_t} \frac{dS_t}{4\pi k |\vec{r}_{i,j} - \vec{r}_t|} \\ i, n = 1, \dots, 3; \quad j, m = \dots, N_{L_i}, N_{L_n}$$

$$\frac{\lambda_{I_s}}{k} + 2K \left[ \begin{array}{l} \sum_{n,m} \lambda_{L_{n,m}} \int_{L_{n,m}} \frac{1}{4\pi\sigma_n} \vec{\nabla} \left( \frac{1}{|\vec{r}_{n,m} - \vec{r}_s|} \right) \cdot \vec{n} \cdot dL_{n,m} + \\ \sum_{t \neq s} \lambda_{I_t} \int_{I_t} \frac{1}{4\pi k} \vec{\nabla} \left( \frac{1}{|\vec{r}_s - \vec{r}_t|} \right) \cdot \vec{n} \cdot dS_t \end{array} \right] = 0 \\ s, t = 1, \dots, N_S \quad (7)$$

where,  $V_{i,j}$  is the potential on the segment  $j$  of the conductor  $C_i$  treated as a thin wire. Vectors  $\vec{r}_{i,j}$  defining the field point position on the surface of the segment  $j$  of the conductor  $C_i$ ,  $\vec{r}_{n,m}$  defining the source point position on the axis of the segment  $m$  of the conductor  $C_n$  and single indexed vectors as  $\vec{r}_s$  defining the position (centre) of the triangular patch labelled  $I_s$ . The system of  $N_{L_1} + N_{L_2} + N_{L_3} + N_S$  equations is completed with other electrical conditions of the conductor system, namely, equal potential of all the conductors and the electric current delivered to the ground by the whole electrode system I, which is distributed among the three electrodes involved namely, the current flowing through the platform  $I_1$ , the current flowing through the tower foundation electrode  $I_2$  and the current flowing through the grounding electrode  $I_3$  as shown in Fig. 5.

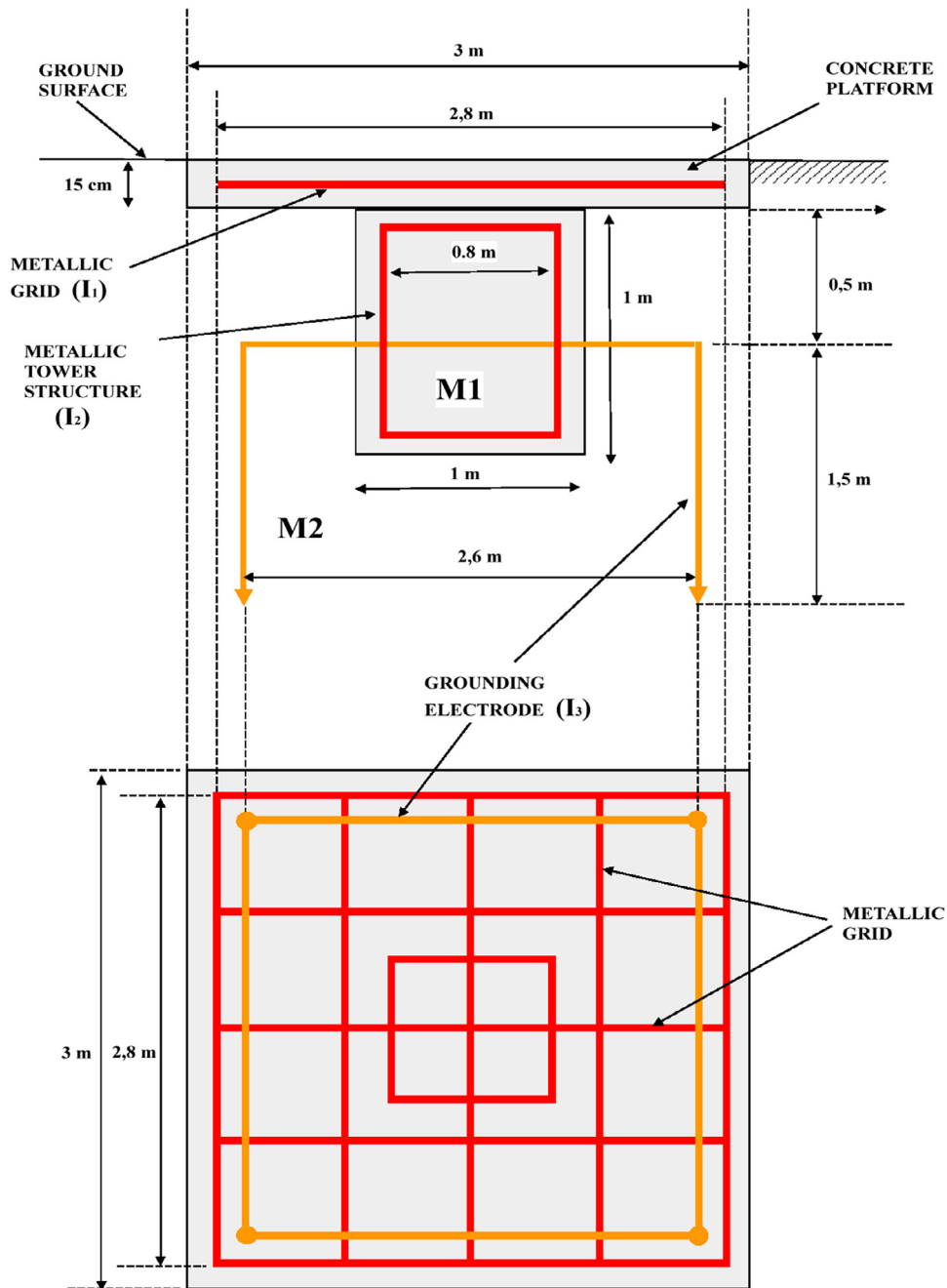


Fig. 5. General plan of the proposed model together with the value of some of the most important lengths.

The numerical procedure has been implemented using an algorithm written in Matlab by the authors, creating the appropriate functions for the electrode segmentation and interface meshing, which contain arguments to control the size of the linear segments and triangular patches for the estimation of errors.

#### 4. Results of the simulation

As noted in the previous section, we will perform the simulation using as standard value for  $\rho_2 = 1 \Omega \text{ m}$  and considering  $K_\rho$  values ranging from 1 to 100. For each selected  $K_\rho$  value, the asymptotic value of the common electrode potential is determined, since due to refinement of the mesh interface and electrode segmentation, such potential shows a significant variability.

Since the total current is set at 1 A, the common potential is normalized according to  $K_V = V/\rho_2 I$  whose value allows the calculation of the potential for a given value of resistivity values ratio. As an example, Table 1 shows the results of the performed simulation for  $K_\rho = 15$ , a typical ratio used in the frame of the aforementioned TABÓN Project. The table shows the currents flowing through the platform  $I_1$ , the tower foundation electrode  $I_2$  and the grounding electrode  $I_3$ , as well as the normalized common potential  $K_V$ . The segmentation of the conductive thin wires were set for convenience to  $M = 30$  segments for each rectilinear element of the conductor. Although the length of the rods is not the same and therefore the segments do not have the same length, the segment size is not relevant as will be seen below. In each row of Table 1, the number of triangular patches of the interface  $N_{\text{tri}}$  is given and the current delivered by each electrode, the normalized common potential  $K_V$

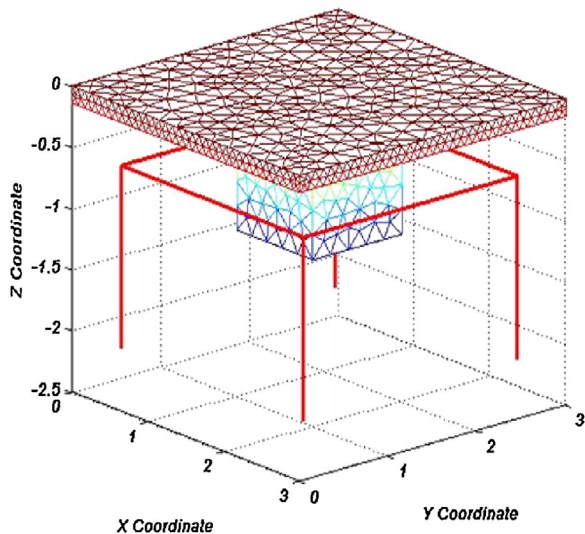


**Fig. 6.** The mesh of the interface separating the two media with different electrical properties at the resolution given by  $N_{\text{tri}} = 1852$  triangles. Only the ground electrode is shown while the remainder of metallic parts are hidden inside the concrete meshed structure.

**Table 1**

Normalized common potential  $K_V$  and leakage currents of the tree electrodes involved in the model: the platform  $I_1$ , the tower foundation  $I_2$  and the grounding electrode  $I_3$  for  $K_\rho = 15$  at a given interface meshing characterised by the number of triangles  $N_{\text{tri}}$  that cover the interface surface.

$N_{\text{tri}}$	$I_1$	$I_2$	$I_3$	$K_V$
1852	0.08559	0.03138	0.88304	0.1141
2170	0.08468	0.03128	0.88405	0.1151
2526	0.08459	0.03090	0.88451	0.1156
2746	0.08430	0.03082	0.88487	0.1159
2988	0.08393	0.03074	0.88533	0.1164
3518	0.08324	0.03064	0.88612	0.1170
4190	0.08286	0.03071	0.88643	0.1173
4610	0.08260	0.03072	0.88668	0.1176
4978	0.08236	0.03070	0.88694	0.1178

Electric currents are given in Amperes, and normalized potential  $K_V$  in  $\text{m}^{-1}$ .

**Table 2**

Potential and leakage current of the main grounding electrode at a given wire segmentation of  $M$  pieces per length of straight wire for  $K_\rho = 15$ .

$M$	$I_3$	$K_V$
30	0.88405	0.11506
50	0.88411	0.11502
70	0.88415	0.11500
90	0.88417	0.11498

Electric current is given in Amperes and normalized potential  $K_V$  in  $\text{m}^{-1}$ .

of the whole grounding electrode system, is obtained as a result of the simulation. As were mentioned above and according to [7], refinement in the mesh interface must lead to the asymptotic value of the normalized common potential  $K_V$ , making it possible to evaluate the error committed by taking a specific meshing in terms of the value of  $N_{\text{tri}}$ .

The effect of refinement in the segmentation of the thin wire electrodes on the values of the above table, is included in Table 2. As an example, starting with an interface meshing composed by  $N_{\text{tri}} = 2170$  pieces, we considered four different segmentations of the thin wires that conform the structure of the embedded grid platform and the model of the metal base of the tower itself. Partitions with  $M = 30, 50, 70$  and  $90$  segments per rectilinear element shall be considered.

Table 2 shows only the leakage current associated to the grounding electrode and the normalized common potential. As can be seen, a weak dependence of the electrical parameters on the number of segments in which the electrodes are divided is found. This effect is not significant, and therefore the analysis will be focused on the dependency of the mesh interface refinement. For this purpose, in order to obtain a representative value of the normalized common potential, a fit of  $K_V$  versus the number of triangles  $N_{\text{tri}} = x$  of the interface has been made by using the second degree rational function,

$$K_V = \frac{ax^2 + bx + c}{x^2 + dx + e} \quad (8)$$

Using a function of this type, it is easy to estimate such a representative value of  $K_V$ , here also called asymptotic value, when refinement is taken to the limit. The coefficient “ $a$ ” from Eq. (8), gives us the sought asymptotic value. Fig. 7 shows such rational fit, obtaining an asymptotic value for the normalized common potential of  $K_V = 0.1200 \text{ m}^{-1}$  in case of  $K_\rho = 15$ . If this  $K_V$  value is multiplied by the actual fault current  $I$ , as well as by the resistivity of the soil  $\rho_2$ , then it matches the grounding resistance in ohms. This asymptotic value also allows an estimate of the error when considering a specific meshing. Taking, for example,  $N_{\text{tri}} = 4978$  pieces, the relative error in  $K_V$  is around 2%.

In order to study the change of  $K_V$  against  $K_\rho$  we must find the asymptotic value of  $K_V$  for each value of  $K_\rho$ , for which a study as shown in Fig. 7 must be made in each case. Table 3 shows the asymptotic values of  $K_V$  according to the value of the parameter  $K_\rho$ . The contents of Table 3 are also graphically represented in Fig. 8. An increase in  $K_V$  with increasing values of  $K_\rho$  is observed,  $K_V$  approaching to an asymptotic value of  $K_V = 0.1247 \text{ m}^{-1}$ , that is, the normalized potential when the platform and tower foundation are made of zero conductivity materials and calculated in a similar way to that employed in the study of  $K_V$  versus  $N_{\text{tri}}$ , but now using a simpler rational expression

$$K_V = \frac{ax + b}{x + c} \quad (9)$$

where,  $K_\rho = x$ .

Taking into account the value of  $K_V = 0.1226 \text{ m}^{-1}$  for the grounding electrode when no other element is present, it can be concluded that the influence of the structural elements of the tower (the tower foundation and the equipotential platform with their respective embedded metallic conductors) on the initially estimated value of the grounding electrode resistance, result in a significant reduction in the grounding resistance of the tower. In case of  $K_\rho = 15$  ( $K_V = 0.1200 \text{ m}^{-1}$ ) it can be initially quantified in a relative decrease of around 2% in the normalized potential, leading to a decrease, to the same extent, in the actual grounding resistance. This percentage increases as  $K_\rho$  decreases, being able to reach up to a 15% decrease in case of  $K_\rho = 1$ . Moreover, the results obtained allow to estimate the changes in the grounding resistance due to possible variations in the resistivities [12] of the involved media by using Eq. (9). Thus, for example, an increase of 10% in the  $K_\rho$  value when this is initially given by  $K_\rho = 3$  leads to a variation of 0.02% in  $K_V$ . However, for this type of tower it is not possible to ignore the effect of the foundation and part of the tower metal structure embedded, as the current flowing through the grounding electrode comes through this structure. Thus, a reference value for  $K_V$ , taking only into account the grounding electrode and the tower metal structure embedded in the concrete block must be calculated. To study it further, some or all conductors embedded in the concrete must be disconnected from the grounding electrode to study again the change  $K_V$  versus  $K_\rho$ . This has been done by the authors by slightly modifying the initial code simulation to allow the presence of independent passive electrodes, which acquire transferred potential with no net

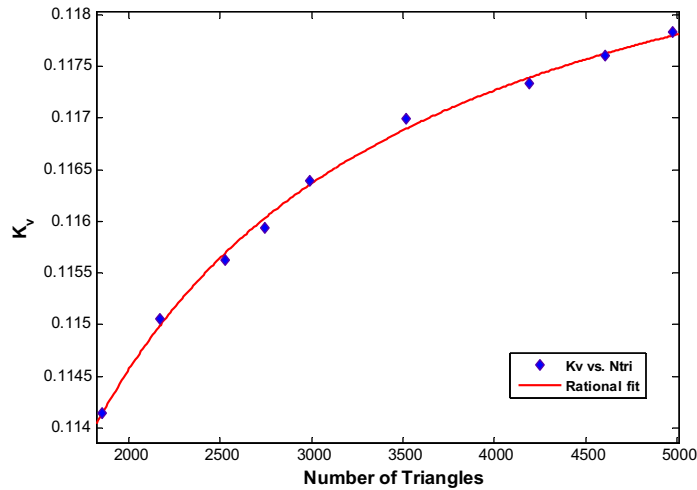


Fig. 7. Rational fit according to Eq. (8), of  $K_V$  in  $m^{-1}$  versus the number of triangles  $N_{tri}$  when  $K_\rho = 15$ .

**Table 3**  
Dimensionless  $K_\rho$  ratio and asymptotic values of the associated normalized potential  $K_V$  in  $m^{-1}$ .

$K_\rho$	1	3	5	7	9	11	13	15	19	25	30	40	100
$K_V$	0.1057	0.1117	0.1147	0.1165	0.1178	0.1187	0.1194	0.1200	0.1208	0.1216	0.1221	0.1227	0.1240

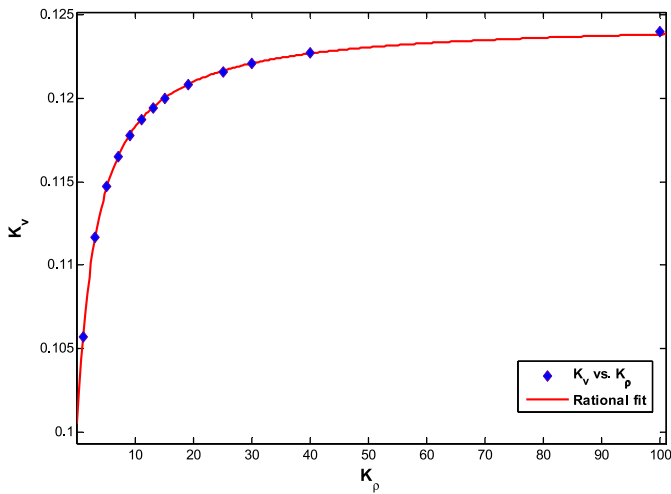


Fig. 8. Rational fit according to Eq. (9), of the asymptotic values of  $K_V$  in  $m^{-1}$  versus the dimensionless parameter  $K_\rho$ . A constant value of  $K_V = 0.1247 m^{-1}$  is reached when  $K_\rho$  tends towards infinity.

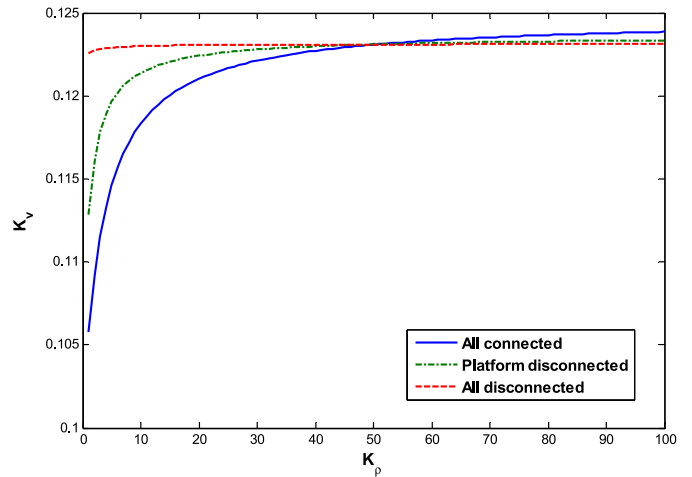


Fig. 9. Asymptotic values of  $K_V$  in  $m^{-1}$  versus the dimensionless parameter  $K_\rho$  for the three electrode configurations. A constant value of  $K_V = 0.1221 m^{-1}$  is reached when  $K_\rho = 15$  in case of the platform is disconnected.

current flow. Fig. 9 shows up to  $K_\rho = 100$ , the variation of  $K_V$  versus  $K_\rho$ , when all the electrodes involved are connected (continuous line), as is also shown in Fig. 8, when the electrode embedded in the platform is disconnected (dash-dotted line) and when all the conductors are all independent while the current flows through the grounding electrode (dashed line). The aforementioned reference value in case of  $K_\rho = 15$  is  $K_V = 0.1221 m^{-1}$ , thus the most realistic relative decrease in the normalized potential is around 1.8%, being able to reach a maximum decrease of 7% when  $K_\rho = 1$ .

The curve shown in Fig. 9 also suggest that it might be advantageous to electrically connect all the structural elements to the grounding system to a certain value of the ratio  $K_\rho$  corresponding to the  $K_V$  value that, keeping in mind the numerical errors, is common to the three configurations which is around  $K_\rho = 50$  for this type of tower. Although the three configurations studied should give the same result for  $K_\rho \rightarrow \infty$ , the fact is that, due to numerical

errors, the asymptotic values differ less than 2%, a result that we believe acceptable.

Fig. 10a shows the potential profile on the ground just above the equipotential platform which surrounds the tower in case of  $K_\rho = 15$ ,  $\rho_2 = 200 \Omega m$  and  $I = 10 A$ . The smoothing effect of the ground potential is clearly visible, although for the mesh size considered, it is far from being really an equipotential platform. However, considering that the structure of the tower rises from the central region of the platform, as shown in Fig. 2, the accessible area of this structure can be certainly considered equipotential.

On the other hand, it would be interesting to see the profile of potential in the bulk soil next to the buried structure under the same electrical conditions. Fig. 10b shows a potential profile in the vertical  $YZ$  plane for  $X = 1.5 m$ , in which is clearly displayed the contour of the interface, thanks to the boundary condition imposed on the normal component of the current density. The figure also clearly shows the profile of the metal grid platform and the points of intersection with the  $YZ$  plane of the rods of the tower structure.

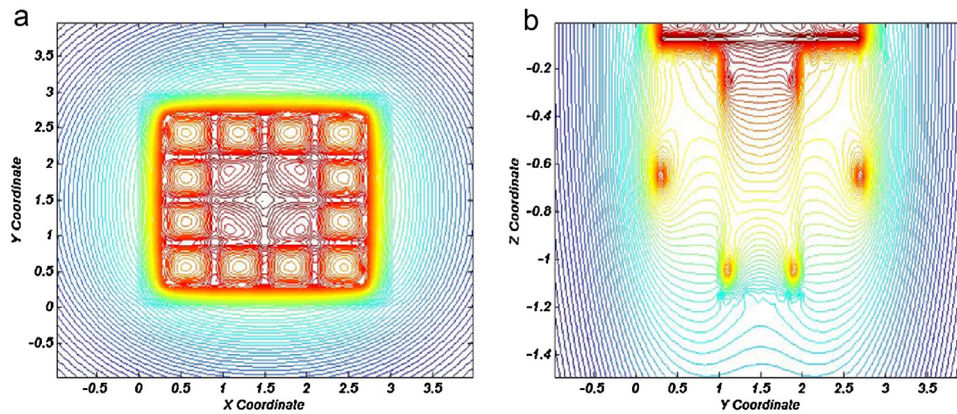


Fig. 10. (a) Ground potential profile over the equipotential platform. (b) Potential profile in the soil on the YZ plane at  $X = 1.5$  m.

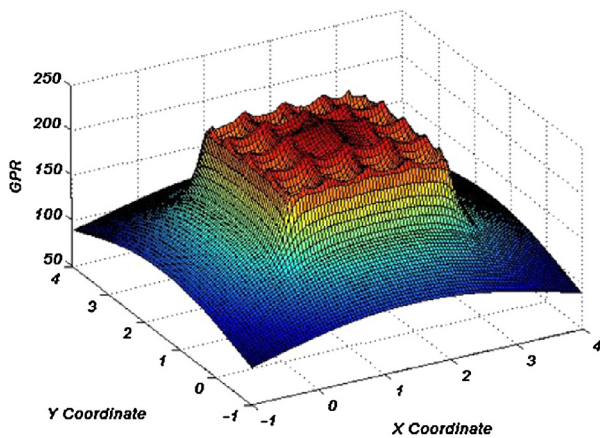


Fig. 11. Surface plot of the ground potential rise.

The cut points with the YZ plane of the grounding electrode are represented by dense yellow points on both sides of the structure. Finally, Fig. 11 shows a surface plot of the ground potential rise on the platform.

For these reasons, initial design specifications of the installation, which initially could only consider the influence of the grounding electrode and possibly the influence of the tower foundation, can be reviewed in order to optimize the design of the installation to account for the possible variation in the initial operating conditions of the grounding system. The possibility of adjusting the size and shape of the grounding electrode could also allow significant cost savings as they may apply to a large number of towers.

Although it is true that there are other factors that significantly alter the grounding resistance of these facilities such as the large variability experienced by the soil resistivity with environmental conditions, temperature, humidity and general climate conditions, the effect of the elements connected to the grounding electrode must be taken into account when optimizing the design and saving unnecessary costs that do not compromise the safety of the installation. As mentioned before, the large number of transmission towers needed in a power line can justify the attempt to get a small savings through the careful choice of grounding electrodes and structural materials that form the foundation and the platform in each of the towers, ensuring in any case a proper operation.

Finally, further research is foreseen to validate all the theoretical calculations in the frame of the aforementioned *TABÓN Project* by means of direct measurements of ground resistance of real electrodes with or without equipotential platform present.

## 5. Conclusions

High voltage transmission line tower are connected to ground by means of electrodes buried in the ground. Classical methods and studies deal with the low frequency grounding resistance and dangerous touch and step voltages calculation taking into account only the buried electrodes, but without considering the effect of other buried elements. In fact, in order to comply with different regulations, especially with touch and step voltage limits, the grounding system is completed by a concrete platform. It is built as an equipotential shallow platform that prevents any dangerous touch voltage. Classical methods do not consider the effect of this platform, the tower foundation, or other structural elements buried in the ground. This paper deals with the effect of the structural buried elements of different resistivity on the grounding resistance and voltage distribution in the ground around the tower. Thus, a simplified model of the grounding system of a power transmission line tower has been proposed and, under certain assumptions, a simulation of its operation by solving Maxwell's equations in inhomogeneous media has been performed. For the special case of piecewise constant media composed of finite volumes of constant conductivities, it is possible to solve the problem with the help of the ESCD model by introducing unknown current distributions on the interface, separating the medium parts with different electrical properties. Original differential equations can be converted into integral equations on the different surfaces, separating the regions with different properties, integral equations that can be solved numerically by the Method of Moments. The main conclusion of this paper is a quantitative estimate of the influence of structural elements, such as the equipotential platform and the tower foundation, on the grounding resistance of the tower when compared with the resistance that would have the grounding system in two different situations: in the absence of any structural element of the installation and, more realistically, when the tower foundation and the embedded metal structure are taken into account. Metallic components embedded in these structures and the material from which they are made, are able to decrease up to between 7% and 15% the theoretical value of the initially calculated grounding resistance. It is also studied the effect on grounding resistance of electrically disconnecting the metal structure of the platform and also to disconnect all metal parts of the system by energizing only the grounding electrode. It is advantageous to interconnect all the metal parts present up to some value of the resistivities ratio from which all settings can be considered equivalent. Although the influence of structural elements may not be the one that most contributes to alter the theoretical value of the grounding resistance, it should not be ignored but, rather added to the set of circumstances that contribute to the high variability found in the measurements

of the grounding resistance of transmission line towers and many other facilities that present conductors embedded in finite volumes with different electrical properties than the bulk of the surrounding medium.

### Acknowledgement

The authors would like to thank the Departments of Electrical Engineering, Applied Mathematics and Applied Physics of the *Escuela Técnica Superior de Ingeniería y Diseño Industrial (ETSIDI)* at Polytechnic University of Madrid (UPM) for their support to the undertaking of the research summarized here. Furthermore, the authors appreciate the useful suggestions and selfless assistance of Prof. A. Vitores. Finally, the authors would like to thank Ms. Gabriela Andres for her contribution to the linguistic correction of the original paper.

### References

- [1] A.P. Meliopoulos, R.P. Web, E.B. Joy, Analysis of grounding systems, *IEEE Trans. Power Appar. Syst.* PAS-100 (3 (March)) (1981) 1039–1048.
- [2] W. Williamson Jr., A problem and its solution involving Maxwell's equations and an inhomogeneous medium, *Am. J. Phys.* 48 (1980) 1063.
- [3] F.P. Dawalibi, W.G. Finney, Transmission line tower grounding performance in non-uniform soil, *IEEE Trans. Power Appar. Syst.* PAS-99 (2 (March/April)) (1980) 471–479.
- [4] H.R. Seedher, J.K. Arora, Estimation of two layer soil parameters using finite werner resistivity expressions, *IEEE Trans. Power Deliv.* 7 (3 (July)) (1992) 1213–1217.
- [5] I. Colominas, F. Navarrina, M. Casteleiro, Numerical simulation of transferred potentials in earthing grids considering layered soil models, *IEEE Trans. Power Deliv.* 22 (3 (July)) (2007) 1514–1522.
- [6] Y.L. Chow, J.J. Yang, K.D. Srivastava, Grounding resistance of buried electrodes in multi-layer earth predicted by simple voltage measurements along earth surface—a theoretical discussion, *IEEE Trans. Power Deliv.* 10 (2 (April)) (1995) 707–715.
- [7] J. Ma, F.P. Dawalibi, Analysis of grounding systems in soils with finite volumes of different resistivities, *IEEE Trans. Power Deliv.* 17 (2 (April)) (2002) 596–702.
- [8] A. Canova, G. Gruosso, 3D source simulation method for static fields in inhomogeneous media, *Int. J. Numer. Methods Eng.* 70 (2007) 1096–1111.
- [9] H.H. Pham, A. Nathan, An integral equation of the second kind for computation of capacitance, *IEEE Trans. Comput. Aided Des. Integr. Circuits Syst.* 18 (10 (Oct.)) (1999) 1435–1441.
- [10] S.M. Rao, T.K. Sarkar, R.F. Harrington, The electrostatic field of conducting bodies in multiple dielectric media, *IEEE Trans. Microw. Theory Tech.* MTT-32 (11 (Nov.)) (1984) 1441–1448.
- [11] J. Tausch, J. White, Capacitance extraction of 3D conductor systems in dielectric media with high-permittivity ratios, *IEEE Trans. Microw. Theory Tech.* 47 (1 (Jan.)) (1999).
- [12] A. Samouelian, I. Cousin, A. Tabbagh, A. Bruand, G. Richar, Electrical resistivity survey in soil science: a review, *Soil Tillage Res.* 83 (2005) 173–193.
- [13] R.F. Harrington, *Field Computation by Moment Methods*, IEEE Press, New York, 1993.
- [14] W.C. Gibson, *The Method of Moments in Electromagnetics*, Chapman & Hall/CRC, 2008, Taylor & Francis Group 6000 Broken Sound Parkway NW, Suite 300 Boca Raton, FL 33487–2742.